Edge ICRF Simulations in 3D Geometry: From MHD Equilibrium to Coupling Determination

G. Suárez López[1,2,a)], M. Cianciosa[3], M. Dunne[1], T. Lunt[1], R. Ochoukov[1], S. K. Seal[3], E. Strumberger[1], W. Tierens[1], M. Willensdorfer[1], H. Zohm[1,2], the ASDEX Upgrade Team[*] and the EUROfusion MST1 Team[†]

[1]*Max Planck Institute for Plasmaphysics, Boltzmannstraße 2, 85748 Garching bei München, Germany.*
[2]*Ludwig-Maximilians-University of Munich, Geschwister-Scholl-Platz 1, 80539 München, Germany.*
[3]*Oak Ridge National Laboratory, Oak Ridge TN, United States of America.*

[a)]Corresponding author: guillermo.suarez@ipp.mpg.de

Abstract. We present in this work a consistent numerical scheme that allows the computation of 3D magnetic fields and 3D density profiles and their usage in ion cyclotron range of frequencies (ICRF) coupling simulations. We first utilize the PARVMEC code to compute the 3D free-boundary plasma equilibrium in the ideal magnetohydrodynamic (MHD) approximation. Since the PARVMEC solution is only defined within the last closed flux surface (LCFS), the magnetic field domain is extended to the scrape-off layer (SOL) via the BMW code, which computes a divergence-free magnetic field solution arising from the external conductors' vacuum field and the PARVMEC flux surface currents. This magnetic reconstruction is then used in the EMC3-EIRENE transport code in order to compute 3D density profiles. In the last step, the RAPLICASOL code is utilized to compute the ICRF antenna S-matrices resulting from the 3D density profiles. We exemplify this scheme for the ASDEX Upgrade tokamak. A new implementation of a curved model for the ASDEX Upgrade ICRF 2-strap antenna in RAPLICASOL allows simulations in realistic geometry, without any coordinate transformations.

Introduction

ICRF coupling simulations allow the prediction of antenna performance in terms of power coupling and radio frequency (RF) near fields, important for impurity production studies. Such simulations are commonly performed in slab geometry, such that the toroidal and poloidal density and induction field gradients are neglected. While this approach is quite robust for the study of axisymmetric configurations, such as standard tokamak scenarios [1], its applicability is limited in intrinsic 3D configurations, such as stellarators or MHD perturbed tokamaks. In order to overcome such limitations, and study the impact of poloidal and toroidal asymmetries in front of ICRF antennas, 3D full wave codes, such as RAPLICASOL [2, 3], have been developed in the past years. RAPLICASOL allows the computation of Maxwell equations in a finite element formulation within a vacuum or plasma region, characterized by a dielectric tensor. It is able to handle arbitrary antenna geometries and anisotropic density and magnetic fields. In this paper, we present a numerical scheme used for the consistent calculation of 3D MHD equilibria and density profiles, which aims to exploit RAPLICASOL's ability to handle 3D geometries, for the study of ICRF coupling performance. We utilized the PARVMEC code [4–6] to compute 3D free-boundary plasma equilibria in the ideal MHD approximation. The induction field domain is further extended to the SOL via the BMW code, which computes a divergence-free induction field solution arising from the external conductors' vacuum field and the PARVMEC flux surface currents. This magnetic reconstruction is then used in the EMC3-EIRENE transport code, in order to compute 3D density profiles. In the last step, the RAPLICASOL code is utilized to compute the ICRF antenna S-matrices. A scheme of the numerical workflow including key output quantities can be seen in **figure 1**.

[*]See the author list of: H. Meyer et al. "Overview of physics studies on ASDEX Upgrade". In: *Nucl. Fusion* (2019).
[†]See the author list of: B. Labit et al. "Dependence on plasma shape and plasma fueling for small edge-localized mode regimes in TCV and ASDEX Upgrade". In: *Nucl. Fusion* (2019).

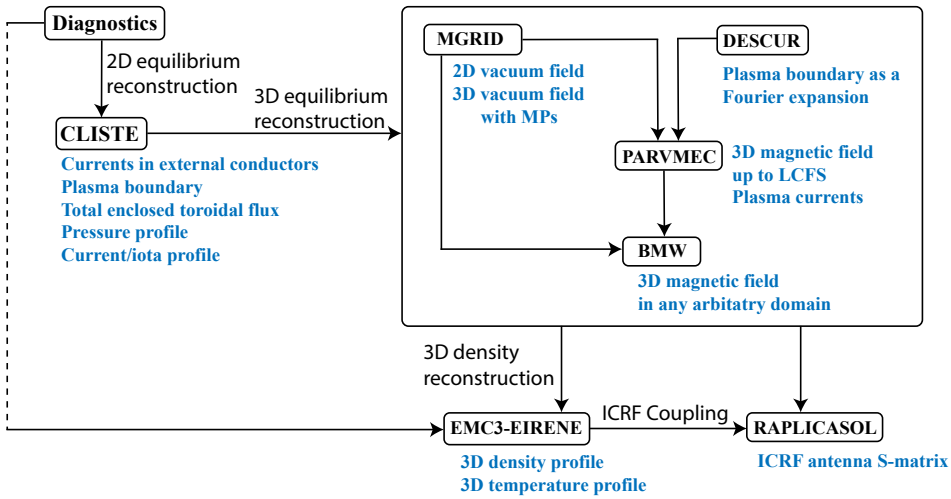

FIGURE 1: Numerical workflow used for the computation of S-matrices in 3D geometry.

MHD modeling

We used ASDEX Upgrade plasma discharge #34632 at $t = 5\,\mathrm{s}$, as the basis for MHD modeling. First, the CLISTE code [7] is utilized to compute an axisymmetric equilibrium solution, constrained by magnetic pick-up coils and the experimentally measured plasma kinetic profiles. The resulting pressure profile, current density and plasma boundary are fed into the PARVMEC code, where we further imposed a 3D field from the magnetic perturbation (MP) coil set [8]. An $n = 2$ toroidally symmetric perturbation field with a current of $I_{\mathrm{MPs}} \sim 3.3\,\mathrm{kA} \times$ turn in the coils, and a differential phase between the upper and lower row of MP coils of $\Delta\varphi_{\mathrm{UL}} = -17.7°$ was applied. The PARVMEC simulation was set with $n = 10$ toroidal harmonics, $m = 28$ poloidal harmonics and $n_s = 1001$ flux surfaces, and a vacuum field resolution of $\{n_r = 256, n_z = 512, n_\phi = 64\}$ points and 2 field periods. The achieved force residual tolerance was $f_{\mathrm{tol}} = 5 \times 10^{-11}$. Next, we input the PARVMEC solution into BMW, in order to evaluate the divergence-free resulting induction field inside and outside the LCFS. This is done by a linear superposition of the vacuum magnetic vector potential and the one generated by the plasma currents, such that:

$$\vec{A}_T(\vec{r}) = \frac{\mu_0}{4\pi} \iiint_{\Omega_p} \frac{\vec{j}(\vec{r}\,')}{|\vec{r} - \vec{r}\,'|} d^3\vec{r}\,' + \vec{A}_v(\vec{r}) \tag{1}$$

Where $\vec{A}_T$ is the *total* (complete domain) magnetic vector potential computed as the superposition of the plasma currents volume integral inside the LCFS, and the vacuum field one, $\vec{A}_v$. The total induction field is then computed by taking the curl: $\vec{B}_T = \vec{\nabla} \times \vec{A}_T$. If the PARVMEC solution were to be perfect, the resulting induction field would display an array of perfectly nested flux surfaces inside the confined region, Ω_p. However, there exist reasons why the PARVMEC solution can fail to represent a given plasma equilibrium within the classical ideal MHD framework. (i): the mathematical representation of flux surface coordinates and field components is given as a Fourier expansion with a finite number of poloidal and toroidal harmonics. This number cannot unfortunately be made arbitrarily large, thus hampering the achievable accuracy. (ii): The ideal MHD solution can be preserved in three-dimensional equilibria when delta-like and Pfirsch-Schlüter currents develop at the rational flux surfaces [9, 10], which are only asymptotically resolved in PARVMEC [11]. For these reasons, magnetic islands and stochastic regions are expected to appear across rational surfaces, where shielding is imperfect, once the plasma solution is superimposed with the original vacuum field. A Poincaré plot of the aforementioned plasma discharge can be found in **figure 2**. We observe that a set of $n = 2$ islands spanning several rational flux surfaces appears. In the plot, we have marked those corresponding to $(m, n) = (5, 2)$, $(6, 2)$ and $(8, 2)$. Furthermore, the LCFS obtained from field-line tracing does not fully correspond to that originally computed by PARVMEC. Nevertheless, the full perturbed equilibrium is recovered, and the plasma 3D displacements are translated along from the MHD calculation to the final induction field, as it will be shown in the next section.

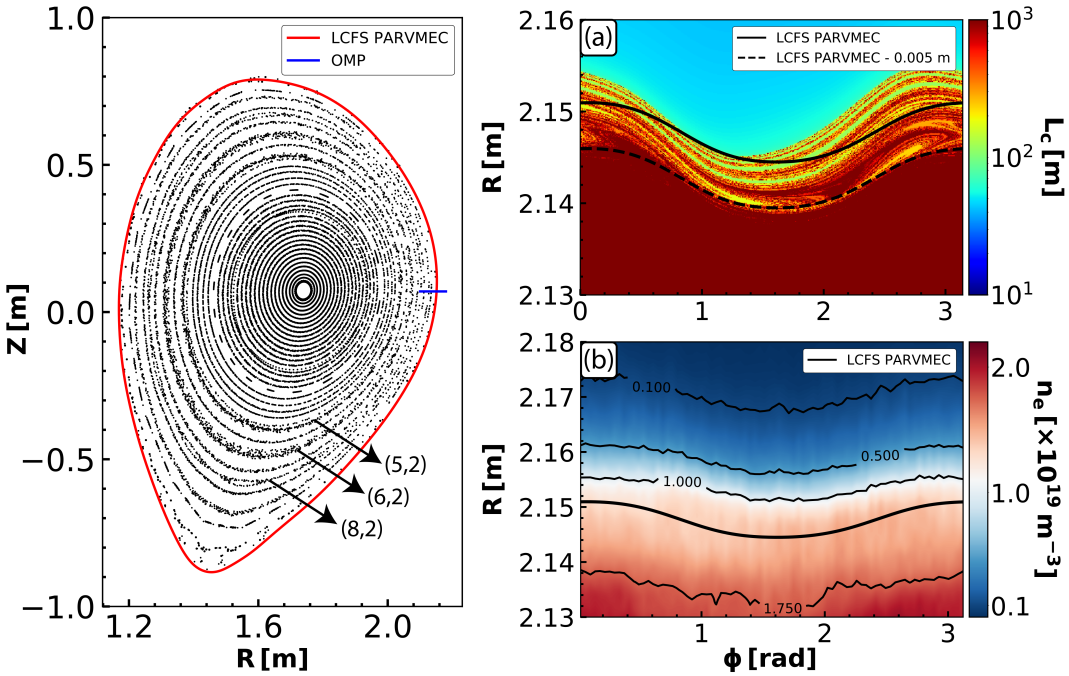

FIGURE 2: Left: Poincaré plot of the PARVMEC&BMW total induction field. Field lines were traced with the GOURDON code [12]. Right: (a) Connection length, L_c, plot projected onto the OMP. (b) EMC3-EIRENE electron density profile, n_e, projected onto the OMP. Only one field period is displayed.

Density profile reconstruction. RAPLICASOL ICRF coupling simulations

We applied the fluid plasma - kinetic neutrals EMC3-EIRENE transport code [13] for the reconstruction of plasma kinetic profiles. A 3D computational grid is constructed on the basis of the total induction field from the PARVMEC&BMW calculation, which is then imported and used in EMC3-EIRENE. As a first technical test, a Monte-Carlo simulation assuming constant plasma background and reflecting boundaries showed a uniform probability density distribution. This so-called "Monte Carlo test" confirms that the numerical violation of $\vec{\nabla} \cdot \vec{B} = 0$ across the LCFS is negligible, and thus the induction field can be used to produce meaningful plasma kinetic profiles. The simulation was set with generic input parameters, i.e., power balance $P_{\text{heat}} - P_{\text{rad}} = 2\,\text{MW}$, separatrix electron density $n_e^{\text{sep}} = 1.5 \times 10^{19}\,\text{m}^{-3}$, particle cross-field diffusion coefficient $D_\perp = 0.2\,\text{m}^2/\text{s}$ and heat cross-field diffusion coefficients $\chi_\perp^e = \chi_\perp^i = 0.6\,\text{m}^2/\text{s}$. The plasma kinetic profiles are then computed. A comparison between the connection length and the obtained density profile at the outboard midplane (OMP) is shown in **figure 2**. The total induction field correctly preserves the PARVMEC plasma displacements inside the high connection length region, whereas a small island layer of about $\sim 0.5 - 1$ cm is observed, placed around the LCFS. Its origin is related to imperfect shielding at rational flux surfaces, which produces finite island width and superposition of these at the densely populated plasma edge.

The computation of the ASDEX Upgrade 2-strap antenna S-matrices was performed with the finite elements COMSOL based RAPLICASOL code. The 3D density computed by EMC3-EIRENE is imported into RAPLICASOL. The 3D induction field was excluded in these simulations due to performance limitations in the perfectly matched layer (PML), which serves as an absorbing boundary condition. Its impact on RF coupling will be quantified in future studies. We utilize a newly developed curved model of the ASDEX Upgrade 2-strap antenna for the simulations [14]. Each of the seven runs performed was set by toroidally shifting the 3D density profile in 22.5° steps, thus effectively rotating it in front of the ICRF antenna. The intent is to reproduce the expected coupling change when MPs are rigidly rotated, already experimentally reported in the literature [15, 16]. The resulting loading resistance in each antenna port is shown in **figure 3**. It is observed that the loading resistance oscillates locked to the density profile, agreeing satisfactorily with the reported experimental behavior. The largest loading resistance value is observed at $\phi \sim 22.5°$, in agreement with the closest approach of the LCFS at the OMP to the ICRF antenna in **figure 2**. The minimum loading resistance is observed at $\phi \sim 112.5°$, corresponding to the largest OMP LCFS-antenna gap distance.

Conclusions and outlook

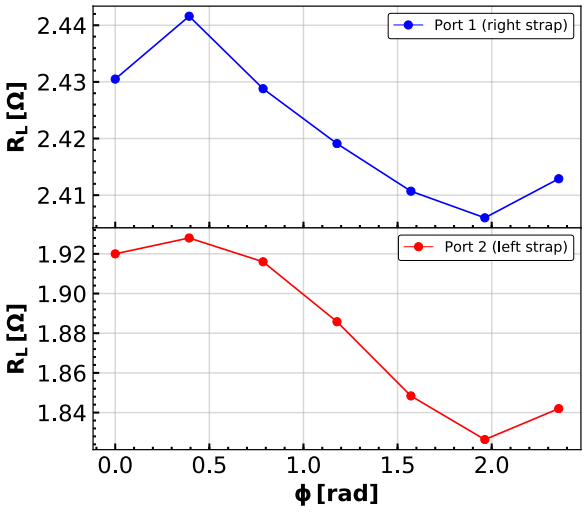

FIGURE 3: Loading resistance per port as computed by RAPLICASOL with the EMC3-EIRENE 3D density profile.

We have successfully utilized the PARVMEC and BMW codes for the simulation of a 3D magnetically perturbed ASDEX Upgrade discharge. To our knowledge, it is the first time that simulations employing together these two codes are reported with tokamak equilibria (whereas they have already been employed for the W7-X stellarator [17]). This code combination has allowed us to reconstruct the magnetic induction field inside and outside the LCFS simultaneously. This is achieved as a linear superposition of the vacuum field, created by the external conductors, with the field generated by the plasma currents, computed by PARVMEC. The resulting total induction field preserves the topological PARVMEC features, but also displays magnetic islands where the provided shielding is insufficient. This field has been satisfactorily input into the EMC3-EIRENE code, where the computation of plasma kinetic profiles has been made possible. These kinetic profiles have served to study the effect of MHD induced 3D asymmetries in the density profiles on the coupling performance of the ASDEX Upgrade 2-strap ICRF antennas. In the future, we expect to quantitatively benchmark this numerical scheme against experimental 3D magnetically perturbed scenarios in ASDEX Upgrade. The proof of principle here provided should also be attractive for ICRF coupling studies in stellarators. For instance, the developed numerical workflow could be used to study the impact of different magnetic configurations on the antenna performance, and should be applicable to W7-X, LHD, etc.

Acknowledgment

This work has been carried out within the framework of the EUROfusion Consortium and has received funding from the Euratom research and training program 2014-2018 and 2019-2020 under grant agreement No 633053. The views and opinions expressed herein do not necessarily reflect those of the European Commission.

References

1. I. Stepanov. “Ion Cyclotron Range of Frequencies (ICRF) Power Coupling and Plasma Density Profile”. PhD thesis. Ghent University, 2015.
2. L. Colas et al. In: *EPJ Web of Conferences* **157** (2017), p. 01001.
3. W. Tierens et al. In: *Nuclear Fusion* **59**.4 (2019), p. 046001.
4. S. P. Hirshman and J. C. Whitson. In: *Physics of Fluids* **26**.12 (1983), p. 3553.
5. S. P. Hirshman, W. I. van RIJ, and P. Merkel. In: *Computer Physics Communications* **43**.1 (1986), pp. 143–155.
6. S. K. Seal et al. In: *Proceedings of the International Conference on Parallel Processing* **2016-Septe** (2016), pp. 618–627.
7. P. J. McCarthy, P. Martin, and W. Schneider. *The CLISTE interpretive equilibrium code*. Tech. rep. Max-Planck-Institut für Plasmaphysik, Garching, 1999.
8. W. Suttrop et al. In: *Plasma Physics and Controlled Fusion* **53**.12 (2011).
9. P. Helander. In: *Reports on Progress in Physics* **77**.8 (2014).
10. J. Loizu et al. In: **022501**.2015 (2015).
11. S. A. Lazerson et al. In: *Physics of Plasmas* **23**.1 (2016).
12. E. Strumberger et al. In: *Nuclear Fusion* **42**.7 (2002), pp. 827–832.
13. Y. Feng et al. In: *Contributions to Plasma Physics* **44**.1-3 (2004), pp. 57–69.
14. W. Tierens et al. In: *This Conference* (2019).
15. G. Suárez López et al. In: *EPJ Web of Conferences* **157** (2017), p. 03051.
16. G. Suárez López et al. In: *Plasma Physics and Controlled Fusion* **61** (2019), p. 125019.
17. J. D. Lore et al. In: *IEEE Transactions on Plasma Science* **46**.5 (2017), pp. 1387–1392.